

Geology

Probing large intraplate earthquakes at the west flank of the Andes

G. Vargas, Y. Klinger, T.K. Rockwell, S.L. Forman, S. Rebolledo, S. Baize, R. Lacassin and R. Armijo

Geology published online 17 October 2014;
doi: 10.1130/G35741.1

Email alerting services click www.gsapubs.org/cgi/alerts to receive free e-mail alerts when new articles cite this article

Subscribe click www.gsapubs.org/subscriptions/ to subscribe to *Geology*

Permission request click <http://www.geosociety.org/pubs/copyrt.htm#gsa> to contact GSA

Copyright not claimed on content prepared wholly by U.S. government employees within scope of their employment. Individual scientists are hereby granted permission, without fees or further requests to GSA, to use a single figure, a single table, and/or a brief paragraph of text in subsequent works and to make unlimited copies of items in GSA's journals for noncommercial use in classrooms to further education and science. This file may not be posted to any Web site, but authors may post the abstracts only of their articles on their own or their organization's Web site providing the posting includes a reference to the article's full citation. GSA provides this and other forums for the presentation of diverse opinions and positions by scientists worldwide, regardless of their race, citizenship, gender, religion, or political viewpoint. Opinions presented in this publication do not reflect official positions of the Society.

Notes

Advance online articles have been peer reviewed and accepted for publication but have not yet appeared in the paper journal (edited, typeset versions may be posted when available prior to final publication). Advance online articles are citable and establish publication priority; they are indexed by GeoRef from initial publication. Citations to Advance online articles must include the digital object identifier (DOIs) and date of initial publication.

Probing large intraplate earthquakes at the west flank of the Andes

G. Vargas^{1*}, Y. Klinger², T.K. Rockwell³, S.L. Forman⁴, S. Rebolledo¹, S. Baize⁵, R. Lacassin², and R. Armijo²

¹Departamento de Geología, CEGA (Andean Geothermal Center of Excellence), Facultad de Ciencias Físicas y Matemáticas, Universidad de Chile, Plaza Ercilla 803, 8370450 Santiago, Chile

²Institut de Physique du Globe de Paris, Sorbonne Paris Cité, Université Paris Diderot, UMR 7154 CNRS, 1 rue Jussieu, F-75005 Paris, France

³Department of Geological Sciences, MC 1020, San Diego State University, San Diego, California 92182, USA

⁴Department of Geology, Baylor University, One Bear Place #97354, Waco, Texas 76798-7354, USA

⁵Institut de Radioprotection et de Sûreté Nucléaire, BP 17, 92262 Fontenay-aux-Roses, France

ABSTRACT

Estimating the potential for the occurrence of large earthquakes on slow-slip-rate faults in continental interiors, away from plate boundaries, is possible only if the long-term geological record of past events is available. However, our knowledge of strong earthquakes appears to be incomplete for thrust faults flanking large actively growing mountain ranges, such as those surrounding Tibet and the Andes Mountains. We present a paleoseismic study of a prominent fault scarp at the west flank of the Andes in Santiago, Chile. The evidence demonstrates recurrent faulting with displacement of ~5 m in each event. With two large earthquake ruptures within the past 17–19 k.y., and the last event occurring ~8 k.y. ago, the fault appears to be ripe for another large earthquake (moment magnitude, M_w 7.5). These results emphasize the potential danger of intraplate continental faults, particularly those associated with youthful mountain fronts.

INTRODUCTION

The largest earthquakes on Earth (moment magnitude, M_w 8–9; Hanks and Kanamori, 1979) are generated by fault rupture at major plate boundaries, generally in subduction zones, producing regionally widespread destruction. However, rupture of secondary fault zones associated with internal deformation of plates and located closer to populated areas can produce intense local destruction in major cities, even if those events are of moderate to large magnitude ($M_w \sim 7$) (Dolan et al., 1995; Rubin et al., 1998; Bilham, 2009; Ritz et al., 2012). An example is the catastrophic 1995 M_w 6.8 Kobe earthquake in Japan, which killed more than 6000 people (Kanamori, 1995). Tragically, the hazard associated with those killer events has often been correctly assessed after their occurrence. The same problem applies for important secondary thrust faults associated with the generation of frontal relief of mountain belts, especially around active growing orogens like Tibet and the Andes Mountains of South America. Again, the importance of the potential hazard of the Long Men Shan thrust, located at the eastern flank of Tibet, was dismissed (Clark et al., 2005) prior to its nearly complete rupture in 2008 that produced the M_w 7.9 Wenchuan earthquake (Xu et al., 2009).

The Chilean subduction margin of South America has produced some of the largest earthquakes worldwide (Cifuentes and Silver, 1989; Vigny et al., 2011). However, the neighboring topographic relief of the Andean orogen is not directly associated with subduction processes, but was created by secondary frontal thrust systems at major Andean ranges (Armijo et al.,

2010; Brooks et al., 2011). To identify the seismic potential of such thrusts is difficult, because large earthquakes there are much less frequent than on the main plate boundary (typically 100× less). While the potential for large thrust earthquakes along the eastern flank of the Andes is now recognized (Brooks et al., 2011), very few events have been accurately recorded historically, and only some moderate-magnitude events have been recorded instrumentally (Alvarado and Beck, 2006) or in paleoseismological trenches, such as the $M_s \sim 7$ earthquake that destroyed

Mendoza, Argentina, in 1861 (Salomon et al., 2013). On the opposite flank of the orogen, the prominent west Andean thrust (Fig. 1), which has geometry and vergence similar to those of the relatively close subduction plate interface, was identified only recently, and the problem of its seismic potential is starting to be considered (Armijo et al., 2010; Pérez et al., 2013).

Santiago city faces the frontal relief of the Andes associated with emergence of the west Andean thrust along a segment called the San Ramon fault (SRF; Fig. 1). Uplift of the Cordillera Principal by slip of the SRF during the past millions of years has produced the dramatic escarpment that rises to San Ramon peak and the Farellones Plateau, 2.7 km and 2 km, respectively, above the city. The surface trace of the fault is clearly expressed by a semicontinuous scarp that extends north to south for at least 35–40 km, from Río Mapocho to south of Río Maipo (Fig. 1) (Armijo et al., 2010). However, the uplift of the high Andes fold-thrust belt extends much farther to the north and south of the emerging trace of the SRF at the edge of the Santiago basin, where the city has expanded,

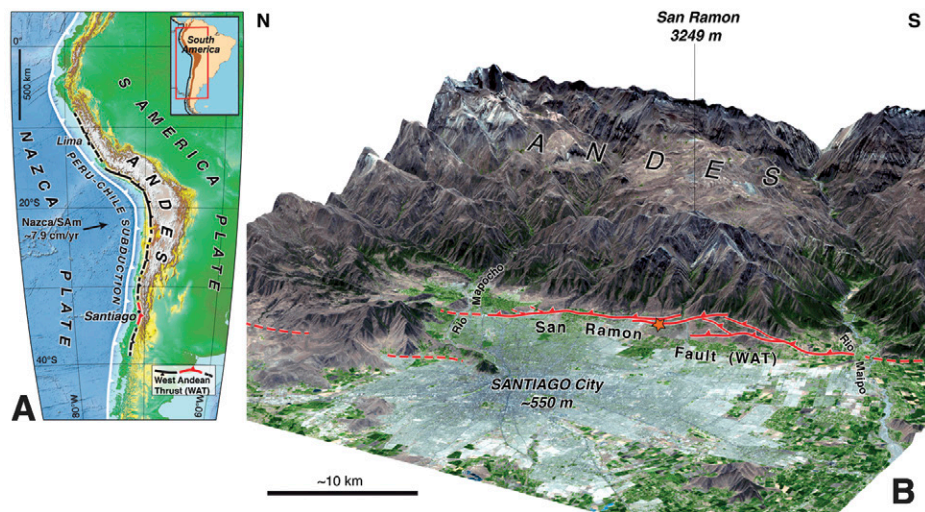


Figure 1. Extent of the west Andean thrust (WAT; Armijo et al., 2010), South America (SAM). A: The WAT is the main active continental-scale fault system at the western foot of the Andes, breaking the west margin of the continent ~200 km eastward from the trench. The Santiago segment of the WAT is in red, and other parts are in black (dashed where less certain). B: Three-dimensional view of Santiago conurbation (more than six million inhabitants) and fault scarps at the piedmont of the abrupt Andean mountain front [SPOT satellite image draped over 30 m digital elevation model, courtesy of Centre National d'Etudes Spatiales]. Orange star shows location of paleoseismological trench.

*E-mail: gvargas@ing.uchile.cl

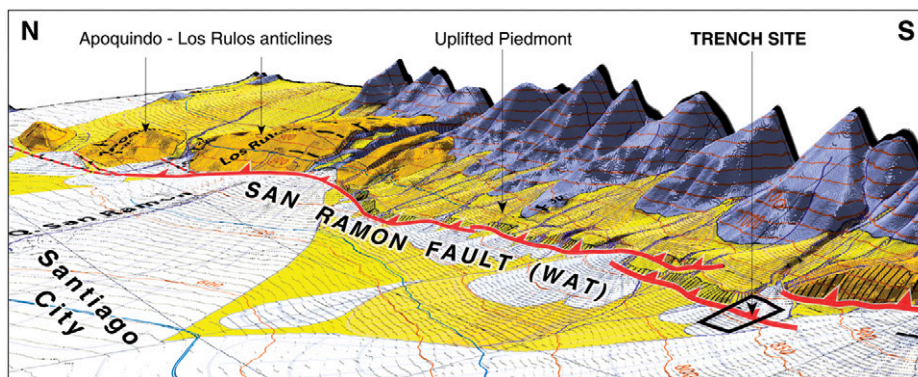


Figure 2. The San Ramón fault scarp, Chile (WAT—west Andean thrust). The geomorphologic map (Armijo et al., 2010) is draped over a 9 m digital elevation model. The San Ramón fault forms a continuous scarp that limits to the west the uplifted piedmont covered with Quaternary alluvium and incised by streams (early-middle Pleistocene in yellow tones, late Pleistocene-Holocene in white). Most of the Quaternary surfaces are urbanized.

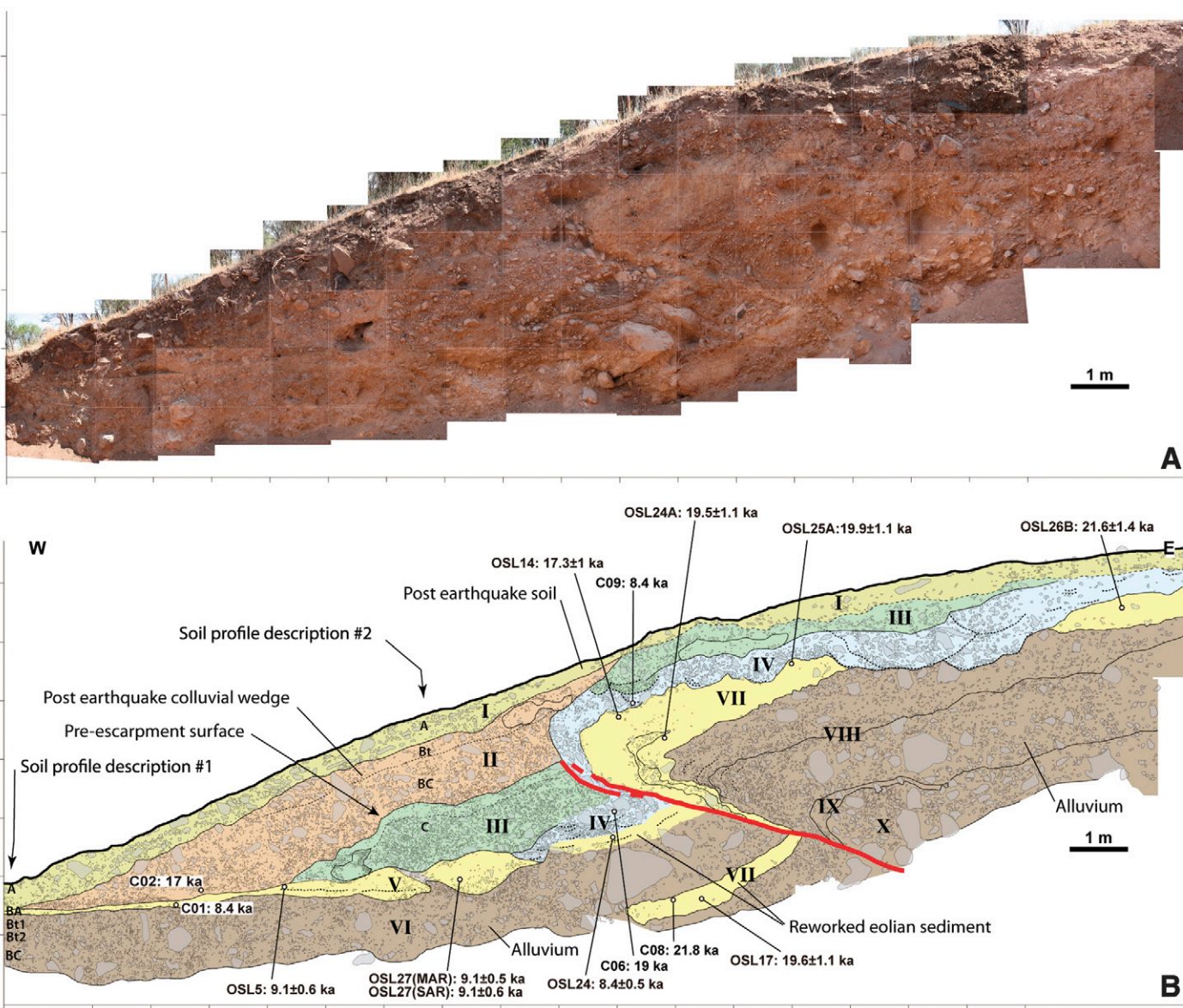


Figure 3. Trench log of the San Ramón fault, Chile. A: Photomosaic of the northern wall of the trench. Each square is 1 m per side. B: Map of northern wall of the trench where units are differentiated according to their content. C0 relates to mean residence time radiocarbon (^{14}C MRT) dates and optically stimulated luminescence (OSL) dates. MAR—multiple aliquot regeneration method; SAR—single aliquot regeneration method.

suggesting that the causative thrust fault system is mostly blind. Here, a paleoseismological study reveals evidence of large intraplate earthquakes in the past 17–19 k.y., demonstrating active tectonic growth of the western flank of the Andes and implying increased seismic risk for the city of Santiago.

PALEOSEISMOLOGICAL TRENCH

The piedmont slopes in the outskirts of Santiago are displaced over a length of ~15 km by Quaternary fault scarps with heights of 3 m to >100 m, marking the clearest emergence of the thrust fault (Fig. 2) (Armijo et al., 2010). From the scarce exposures left intact from recent urbanization, we trenched the morphologically youngest scarp (~3–5 m high) in front of an active drainage in which the most recent fault offsets and associated sediments were preserved in Holocene alluvial fan deposits (Fig. 2).

Despite unfavorable rough sedimentological conditions, a trench 25 m long and 5 m deep (Fig. 3) exposed crucial geometric features of the fault, which displaced and deformed two distinct types of sediments. Units I–IV, VI, and VIII–X are composed of massive, gravelly, fluvial-channel or debris-flow deposits. Unit IV includes evidence for channeling at its base with a distinctive erosional surface. Units V and VII, in contrast, are very well sorted, silt-rich strata that we interpreted to be of eolian origin. Unit V is likely derived from unit VII, based on age relationships described here, and was deposited by colluvial processes after faulting. Unit V emerges from beneath units I–III at the base of the scarp as the modern topsoil horizon.

The coarse nature of most units exposed in the trench limits the dating possibilities to a few critical layers. Unit V yielded consistent optically stimulated luminescence (OSL) and mean residence time radiocarbon (^{14}C MRT) ages ranging from 8.4 to 9.1 kyr B.P. (Fig. 3; see the GSA Data Repository¹). Unit VII also yielded consistent ages ranging from 17.3 to 21.8 kyr B.P. The similarity between the ^{14}C MRT and the OSL dates argues that emplacement of unit V was close to 9 kyr B.P., and emplacement of unit VII was ca. 17–21 kyr B.P. In addition, two soil profiles (Fig. 3; Appendix 1; see the Data Repository) were described that characterize periods of nondeposition and surface stability. From profile 2, we infer that the ground surface above the colluvial wedge has been relatively stable for several thousands of years. These observations are consistent with deposition of units I–V at an age close to that of the OSL and ^{14}C MRT dates obtained from unit V.

¹GSA Data Repository item 2014371, data and dating methodology, Tables DR1–DR6, and Figures DR1–DR56, is available online at www.geosociety.org/pubs/ft2014.htm, or on request from editing@geosociety.org or Documents Secretary, GSA, P.O. Box 9140, Boulder, CO 80301, USA.

The trench exposes evidence for two earthquakes, E1 and E2, that postdate unit VII. Individual coseismic slip is estimated by restoring units into their initial geometry (Fig. 4). Units III and IV, which predate E2, were reconstructed and unfolded, and unit V was matched with unit VII; missing unit III material (Fig. 4) indicates that some of unit III was eroded into unit II that now forms the colluvial wedge associated with E2. The slip resulting from E2 is estimated to be 4.7 m. We correlate the units identified as VII that yielded similar ages and have similar characteristics on both sides of the fault. Because unit IV erodes it, the initial thickness of unit VII in the hanging wall is arguable. This implies a larger uncertainty on E1 coseismic offset, which ranges between 4.2 m and 5.7 m (Fig. 4). The cumulative displacement in two earthquakes on the SRF is estimated with confidence as 8.4–10.9 m, or 9.7 ± 1.2 m, about twice the displacement estimated for the most recent event, suggesting that each event was similar in size and close to 5 m (Fig. 4).

EARTHQUAKE ESTIMATES AND IMPLICATIONS FOR SEISMIC HAZARD

Using 5 m as the maximum surface displacement, scaling laws (Wells and Coppersmith, 1994) predict $M_w = 7.2$. Alternatively, assuming that 5 m represents the average surface displacement yields $M_w = 7.5$. Seismic moment can also be estimated with a fixed rupture width of 30

km, consistent with the structure of the SRF at depth (Armijo et al., 2010; Pérez et al., 2013) and 5 m of average slip. In that case, assuming that the fault scarp is either 15 km long, according to the most emergent part of the scarp, or 35 km long if considering the entire well-recognized SRF (Armijo et al., 2010), predicts $M_w = 7.25$ and $M_w = 7.5$, respectively.

Those magnitude estimates imply surface rupture and significantly stronger ground motion (and destructive effects) for Santiago than previously proposed (Pérez et al., 2013; Pilz et al., 2011). Seismic hazard is commonly assessed in engineering applications using deterministic and/or probabilistic approaches, by the application of the response spectrum technique. Using acceleration attenuation laws that consider the earthquake fault trace site distance including the near-field region (<25 km) for large crustal earthquakes (Abrahamson et al., 2008), in the case of a deterministic M_w 7.5 scenario, modeled horizontal peak ground acceleration (PGA) in the footwall would reach mean values of 0.5 g, 0.4 g, and 0.3 g at 1 km, 5 km, and 10 km from the SRF, respectively, eventually exceeding 1 g at short distances in the three cases (see the Data Repository). These values are significantly higher, by 4%–80%, than the PGA predicted for the scenario of an earthquake of M_w 6–6.9 along this fault (Pérez et al., 2013; Pilz et al., 2011), and they are higher also than the ~0.2–0.3 g, locally 0.56 g PGA, recorded at Santiago dur-

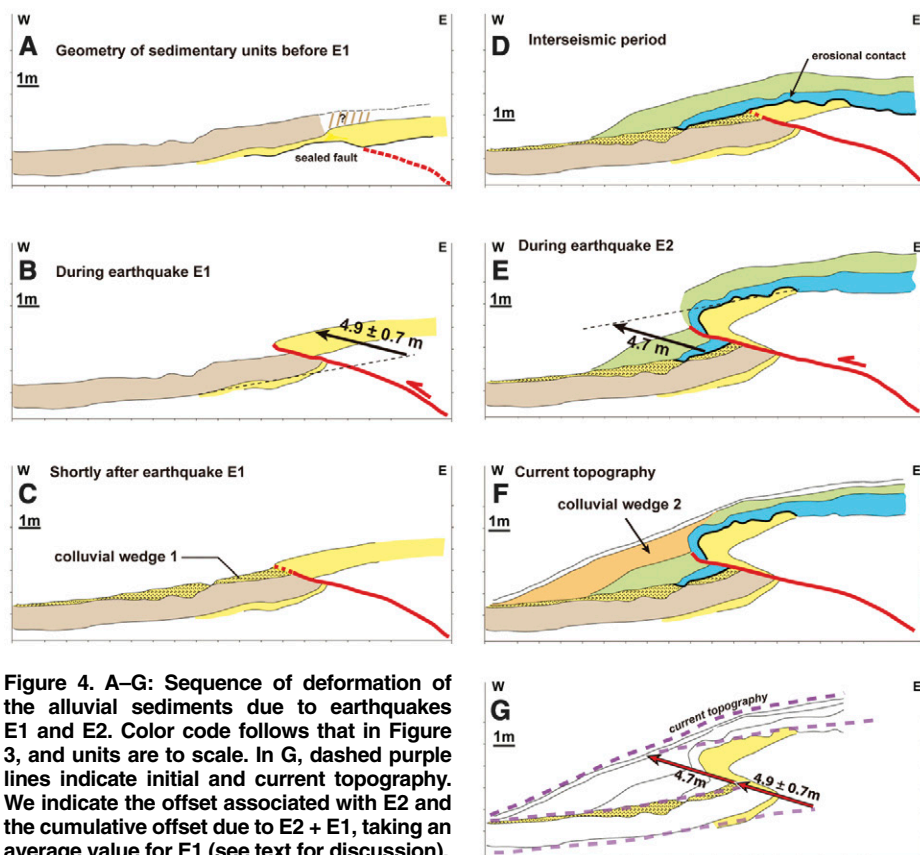


Figure 4. A–G: Sequence of deformation of the alluvial sediments due to earthquakes E1 and E2. Color code follows that in Figure 3, and units are to scale. In G, dashed purple lines indicate initial and current topography. We indicate the offset associated with E2 and the cumulative offset due to E2 + E1, taking an average value for E1 (see text for discussion).

ing the last 2010 M_w 8.8 Maule megathrust rupture (Saragoni et al., 2010). However, all those values should be considered as lower estimates because they do not incorporate possible effects of basin topography or earthquake directivity.

The timing of events E1 and E2 is well constrained; both occurred in the past 17–20 k.y. Interpretation of soil profiles implies that units III and IV are similar in age to unit V, dated at 8–9 k.y. B.P. Consequently, we interpret event E2 to have occurred soon after deposition of unit III, ca. 8 ka; it was followed by deposition of the colluvial wedge associated with unit II, then by surface stability, allowing for the development of soil profile 2. We conclude that the SRF has remained unbroken by large earthquakes comparable with E1 and E2 since ca. 8 ka and that there is no evidence in the trench for rupture associated with historic events from the short seismic catalogs (constrained to a few hundred years and with sparse chronicles that make earthquakes-source discrimination difficult), particularly the large event of A.D. 1647 that heavily damaged Santiago (Lomnitz, 2004; Cisternas et al., 2012). Therefore, dating suggests that the SRF might be due for another large rupture similar to those documented in the trench. A change in stress regime on Andean crustal structures (Scott et al., 2014), like stress concentration near the northern tip of the 2010 M_w ~ 8.8 Maule subduction earthquake, could accelerate processes leading to its next rupture, and puts Santiago at higher risk than previously thought (Bilham, 2009; Stein and Toda, 2013).

CONCLUSIONS

Thrust faults with characteristics very similar to those observed in the SRF are known for having recently produced destructive earthquakes elsewhere around the world, in a variety of tectonic contexts (Ritz et al., 2012; Kanamori, 1995; Xu et al., 2009; Sapkota et al., 2013), so we emphasize the potential danger of an earthquake by rupture of the SRF in Santiago, Chile. With two large (M_w ~ 7.5) earthquakes in the past 17–19 k.y., the evidence in the trench described here proves more generally the young activity of the west Andean thrust, so most of the foregoing could be reasonably extended to any other segment of that structure throughout the Andean west flank. Generalizing further, despite long return times that might give a false sense of security, our study suggests that thrust faults at fronts of any active orogeny should be regarded as potential sources of large destructive earthquakes.

APPENDIX 1. SOIL PROFILES

Santiago is in a semiarid climate zone (~312 mm/yr precipitation), although there has apparently been sufficient rainfall to flush most of the carbonate and other salts from the profile in the trench. We described two pedons (profiles 1 and 2; Fig. 3). Profile 1 is developed in the alluvium and/or colluvium that buries unit VII and is therefore inferred to be between 9 and 17

ka. Profile 2 is developed only in the colluvial wedge that formed after the most recent event, and is therefore younger than 9 ka. Pedon 1 exhibits stronger expression of soil development, with a moderately developed argillic horizon with many secondary clay films, well-developed structure, but no significant reddening. Pedon 2 exhibits soil development similar to, but slightly less than, that of pedon 1. The presence of a moderately developed argillic horizon associated with pedon 2 indicates that the surface has been stable for many thousands of years. We conclude that nearly all of the time locked up in the colluvial wedge that resulted from the most recent event appears to be expressed in the surface soil at pedon 2, with additional time evidenced by the slightly stronger soil profile at pedon 1.

ACKNOWLEDGMENTS

This work was supported by Ministerio de Vivienda y Urbanismo (Seremi Región Metropolitana, Project 640-27-LP10), Gobierno de Chile. Additional support was provided by Millennium Nucleus-Grant P06-064-F, CEGA FONDAP Project 15090013, and the LabEx UnivEarthS and ANR (Agence Nationale de la Recherche, France) MegaChile projects. We thank V. Flores, C. Valderas, and T. Iglesias for field support.

REFERENCES CITED

- Abrahamson, N.A., Atkinson, G., Boore, D., Bozorgnia, Y., Campbell, K., Chiou, B., Idriss, I.M., Silva, W., and Youngs, R., 2008, Comparisons of the NGA ground-motion relations: *Earthquake Spectra*, v. 24, p. 45–66, doi:10.1193/1.2924363.
- Alvarado, P., and Beck, S., 2006, Source characterization of the San Juan (Argentina) crustal earthquakes of 15 January 1944 (M_w 7.0) and 11 June 1952 (M_w 6.8): *Earth and Planetary Science Letters*, v. 243, p. 615–631, doi:10.1016/j.epsl.2006.01.015.
- Armijo, R., Rauld, R., Thiele, R., Vargas, G., Campos, J., Lacassin, R., and Kausel, E., 2010, The West Andean thrust, the San Ramón fault and the seismic hazard for Santiago, Chile: *Tectonics*, v. 29, TC2007, doi:10.1029/2008TC002427.
- Bilham, R., 2009, The seismic future of cities: *Bulletin of Earthquake Engineering*, v. 7, p. 839–887, doi:10.1007/s10518-009-9147-0.
- Brooks, B.A., et al., 2011, Orogenic-wedge deformation and potential for great earthquakes in the central Andean backarc: *Nature Geoscience*, v. 4, p. 380–383, doi:10.1038/ngeo1143.
- Cifuentes, I.L., and Silver, P.G., 1989, Low-frequency source characteristics of the great 1960 Chilean earthquake: *Journal of Geophysical Research*, v. 94, p. 643–663, doi:10.1029/JB094iB01p00643.
- Cisternas, M., Torrejón, F., and Gorigoitia, N., 2012, Amending and complicating Chile's seismic catalog with the Santiago earthquake of 7 August 1580: *Journal of South American Earth Sciences*, v. 33, p. 102–109, doi:10.1016/j.jsames.2011.09.002.
- Clark, M.K., House, M.A., Royden, L.H., Whipple, K.X., Burchfiel, B.C., Zhang, X., and Tang, W., 2005, Late Cenozoic uplift of southern Tibet: *Geology*, v. 33, p. 525–528, doi:10.1130/G21265.1.
- Dolan, J., Sieh, K., Rockwell, T.K., Yeats, R., Shaw, J., Suppe, J., Huftile, G., and Gath, E., 1995, Prospects for larger or more frequent earthquakes in the Los Angeles metropolitan region: *Science*, v. 267, p. 199–205, doi:10.1126/science.267.5195.199.
- Hanks, T.C., and Kanamori, H., 1979, A moment magnitude scale: *Journal of Geophysical Research*, v. 84, p. 2348–2350, doi:10.1029/JB084iB05p02348.

- Kanamori, H., 1995, The Kobe (Hyogo-ken Nanbu), Japan, earthquake of January 16, 1995: *Seismological Research Letters*, v. 66, p. 6–10, doi:10.1785/gssrl.66.2.6.
- Lomnitz, C., 2004, Major earthquakes of Chile: A historical survey, 1535–1960: *Seismological Research Letters*, v. 75, p. 368–378, doi:10.1785/gssrl.75.3.368.
- Pérez, A., Ruiz, J.A., Vargas, G., Rauld, R., Rebolledo, S., and Campos, J., 2013, Improving seismotectonics and seismic hazard assessment along the San Ramón fault at the eastern border of Santiago city, Chile: *Natural Hazards*, v. 71, p. 243–274, doi:10.1007/s11069-013-0908-3.
- Pilz, M., Parolai, S., Stupazzini, M., Paolucci, R., and Zschau, J., 2011, Modelling basin effects on earthquake ground motion in the Santiago de Chile basin by a spectral element code: *Geophysical Journal International*, v. 187, p. 929–945, doi:10.1111/j.1365-246X.2011.05183.x.
- Ritz, J.F., Nazari, H., Balescu, S., Lamothe, M., Salamati, R., Ghassemi, A., Shafei, A., Ghorashi, M., and Saidi, A., 2012, Paleoequakes of the past 30,000 years along the North Tehran fault (Iran): *Journal of Geophysical Research*, v. 117, B06305, doi:10.1029/2012JB009147.
- Rubin, C., Lindvall, S., and Rockwell, T.K., 1998, Evidence for large earthquakes in metropolitan Los Angeles: *Science*, v. 281, p. 398–402, doi:10.1126/science.281.5375.398.
- Salomon, E., Schmidt, S., Hetzler, R., Mingorance, F., and Hampel, A., 2013, Repeated folding during late Holocene earthquakes on the La Cal thrust fault near Mendoza city (Argentina): *Seismological Society of America Bulletin*, v. 103, p. 936–949, doi:10.1785/0120110335.
- Saragoni, G., Lew, M., Naeim, F., Carpenter, L., Youssef, N., and Rojas, F., 2010, Accelerographic measurements of the 27 February 2010 offshore Maule, Chile earthquake: *Structural Design of Tall and Special Buildings*, v. 19, p. 866–875, doi:10.1002/tal.673.
- Sapkota, S., Bollinger, L., Klinger, Y., Tapponier, P., Gaudemer, Y., and Tiwari, D., 2013, Primary surface ruptures of the great Himalayan earthquake in 1934 and 1255: *Nature Geoscience*, v. 6, p. 71–76, doi:10.1038/ngeo1720.
- Scott, C., Lohman, R., Pritchard, M., Alvarado, P., and Sánchez, G., 2014, Andean earthquakes triggered by the 2010 Maule, Chile (M_w 8.8) earthquake: Comparisons of geodetic, seismic and geologic constraints: *Journal of South American Earth Sciences*, v. 50, p. 27–39, doi:10.1016/j.jsames.2013.12.001.
- Stein, R.S., and Toda, S., 2013, Megacity megaquakes—Two near misses: *Science*, v. 341, p. 850–852, doi:10.1126/science.1238944.
- Vigny, C., et al., 2011, The 2010 M_w 8.8 Maule megathrust earthquake of central Chile, monitored by GPS: *Science*, v. 332, p. 1417–1421, doi:10.1126/science.1204132.
- Wells, D.L., and Coppersmith, K.J., 1994, New empirical relationships among magnitude, rupture length, rupture width, rupture area, and surface displacement: *Seismological Society of America Bulletin*, v. 84, p. 974–1002.
- Xu, X., Wen, X., Yu, G., Chen, G., Klinger, Y., Hubbard, J., and Shaw, J., 2009, Co-seismic reverse- and oblique-slip surface faulting generated by the 2008 M_w 7.9 Wenshan earthquake, China: *Geology*, v. 37, p. 515–518, doi:10.1130/G25462A.1.

Manuscript received 2 April 2014

Revised manuscript received 10 September 2014

Manuscript accepted 11 September 2014

Printed in USA